The Astrophysical Journal, 625:L9–L12, 2005 May 20
© 2005. The American Astronomical Society. All rights reserved. Printed in U.S.A.

THE POWERFUL OUTBURST IN HERCULES A

P. E. J. Nulsen,[1,2] D. C. Hambrick,[1,3] B. R. McNamara,[4] D. Rafferty,[4] L. Birzan,[4] M. W. Wise,[5] and L. P. David[1]
Received 2004 December 1; accepted 2005 April 14; published 2005 April 28

ABSTRACT

The radio source Hercules A resides at the center of a cooling flow cluster of galaxies at redshift $z = 0.154$. A *Chandra* X-ray image reveals a shock front in the intracluster medium (ICM) surrounding the radio source, about 160 kpc from the active galactic nucleus (AGN) that hosts it. The shock has a Mach number of 1.65, making it the strongest of the cluster-scale shocks driven by an AGN outburst found so far. The age of the outburst is $\simeq 5.9 \times 10^7$ yr, its energy $\sim 3 \times 10^{61}$ ergs, and its mean power $\sim 1.6 \times 10^{46}$ ergs s^{-1}. As for the other large AGN outbursts in cooling flow clusters, this outburst overwhelms radiative losses from the ICM of the Hercules A Cluster by a factor of ~100. It adds to the case that AGN outbursts are a significant source of preheating for the ICM. Unless the mechanical efficiency of the AGN in Hercules A exceeds 10%, the central black hole must have grown by more than $1.7 \times 10^8\ M_\odot$ to power this one outburst.

Subject headings: cooling flows — galaxies: clusters: individual (Hercules A) — intergalactic medium — X-rays: galaxies: clusters

1. INTRODUCTION

It is not yet clear which heating mechanism (e.g., Narayan & Medvedev 2001; Motl et al. 2004) is chiefly responsible for preventing gas from cooling in cluster cooling flows (Peterson et al. 2003), but the most promising is heating by a central AGN (Tabor & Binney 1993; Tucker & David 1997). Heating and cooling rates are linked if the AGN is fed by cooled or cooling gas. Such feedback could maintain otherwise unstable cool cores, explaining the prevalence of cooling flows (Fabian 1994). AGN-powered radio-lobe cavities (e.g., Carilli et al. 1994; McNamara et al. 2000; Fabian et al. 2000) heat the ICM (Churazov et al. 2002), but not enough to make up for radiative losses (Birzan et al. 2004). Weak "cocoon" shocks, long expected in models of jet-fed radio lobes (e.g., Scheuer 1974; Heinz et al. 1998), have been found in a number of systems (Fabian et al. 2003; Forman et al. 2005; McNamara et al. 2005; Nulsen et al. 2005). They represent additional heating due to AGN outbursts, and they provide a new tool for determining ages and energies of AGN outbursts.

In this Letter, we report the discovery of a shock front generated by the AGN outburst that powers Hercules A. One of the brightest radio sources in the sky (Dreher & Feigelson 1984; Gizani & Leahy 2003), Hercules A resides at the center of a cluster of galaxies with X-ray luminosity $\simeq 5 \times 10^{44}$ ergs s^{-1}, at redshift $z = 0.154$ (Siebert et al. 1999; Gizani & Leahy 2004). Despite its high radio luminosity, Hercules A lacks bright radio hot spots and so belongs to Fanaroff-Riley class I, but with an unusual, jet-dominated, radio morphology (Dreher & Feigelson 1984; Gizani & Leahy 2003). Using *Einstein* spectra, White et al. (1997) found a formal cooling rate of zero for the Hercules A Cluster, but the high central density we find ($n_e \gtrsim 0.1$ cm^{-3}) gives it a central cooling time typical of a cooling flow cluster.

In § 2 we give details of the observations and data reduction, and in § 3 we discuss the main features of the *Chandra* image of Hercules A. Properties of the shock are discussed in § 4, and its implications in § 5. A flat ΛCDM cosmology, with $H_0 = 70$ km s^{-1} Mpc^{-1} and $\Omega_m = 0.3$, is assumed throughout, giving a scale of 2.67 kpc arcsec^{-1} for Hercules A.

2. OBSERVATIONS AND DATA REDUCTION

Hercules A was observed with *Chandra* for 14.8 ks on 2001 July 25, in VFAINT mode with ACIS-S at the aim point (ObsID 1625). For the analysis here, the event list was reprocessed using recent calibrations. It was screened to remove *ASCA* grades 1, 5, and 7 and bad pixels. Periods of high particle background were removed following the method of M. Markevitch,[6] leaving 12.4 ks of good exposure time. After cleaning, the mean count rate in ACIS-S1 was 0.136 counts s^{-1}, ~3.5 σ (9%) higher than expected,[7] suggesting some residual contamination due to particle background. Data were processed to correct for the time dependence of the ACIS gain[8] and filtered according to the prescription of A. Vikhlinin[9] to reduce particle background. Background event files were created by processing standard ACIS background files in the same manner as the data. Point sources were identified manually for removal from spectra and surface brightness profiles. Ancillary response files and response matrix files for extended regions are weighted by number of events. Ancillary response files are corrected to allow for the reduction in low-energy response due to contaminant on the ACIS filters.

3. THE X-RAY IMAGE OF HERCULES A

The image in the upper panel of Figure 1 shows the filtered and calibrated events from the raw *Chandra* data (evt2 file) for Hercules A, binned by a factor of 4. The lower panel shows a 0.3–7.5 keV image made after the cleaning and reprocessing described above. The image has been smoothed with a 2″ Gaussian and divided by a β-model, with a 42″ core radius and a

[1] Harvard-Smithsonian Center for Astrophysics, 60 Garden Street, Cambridge, MA 02138; pnulsen@cfa.harvard.edu.
[2] On leave from the University of Wollongong.
[3] Harvey Mudd College, 301 East Foothill Boulevard, Claremont, CA 91711.
[4] Astrophysical Institute, and Department of Physics and Astronomy, Ohio University, Clippinger Laboratories, Athens, OH 45701.
[5] Center for Space Research, Building NE80-6015, Massachusetts Institute of Technology, Cambridge, MA 02139.

[6] See http://hea-www.harvard.edu/~maxim/axaf/acisbg.
[7] See http://hea-www.harvard.edu/~maxim/axaf/acisbg/data/README.
[8] See http://hea-www.harvard.edu/~alexey/acis/tgain.
[9] See http://cxc.harvard.edu/cal/Acis/Cal_prods/vfbkgrnd.

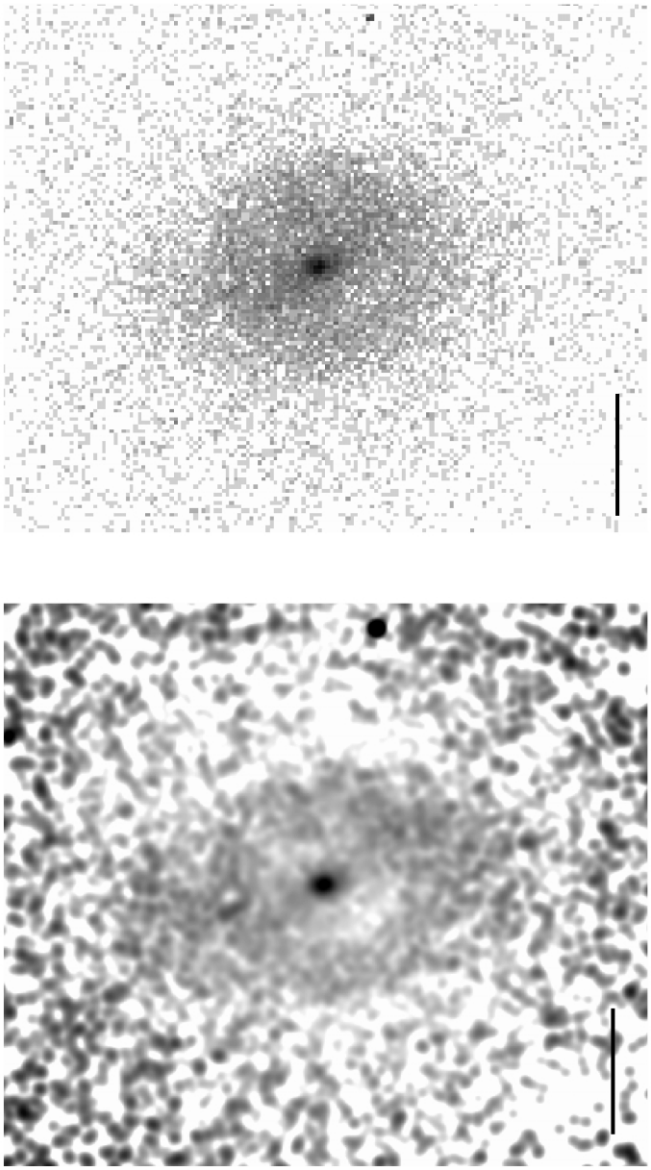

FIG. 1.—*Upper panel:* 0.3–7.5 keV *Chandra* image of Hercules A made from the distributed evt2 file binned by a factor of 4. *Lower panel:* 0.3–7.5 keV image of Hercules A made from the cleaned, reprocessed data, smoothed with a 2″ Gaussian and divided by a β-model. The scale bar in each panel is 1′ (160 kpc) in length. The bright central region ∼1′ in radius is surrounded by the shock front. The southwest cavity is ∼0.′5 from the central peak.

β of 0.6, centered on the X-ray peak (core radius from Gizani & Leahy 2004, but smaller β). Division by the β-model reduces the radial variation of surface brightness, making it easier to discern substructure over a substantial range of radius. Each image has a 1′ scale bar.

Although the central peak of the X-ray image is prominent, it is well resolved by *Chandra*, and there is no sign of a point-like AGN (cf. Trussoni et al. 2001). A striking feature of the X-ray image is the bright region, roughly 1′ in radius, that stands out in the upper panel of Figure 1. This has a similar size to the radio emission and extends to the east and west around the radio lobes (see Fig. 1, *lower panel*, and Fig. 2). Its shape and association with the radio source suggest that it is the shocked cocoon of the expanding radio lobes (Scheuer 1974; Heinz et al. 1998). The break in surface brightness that

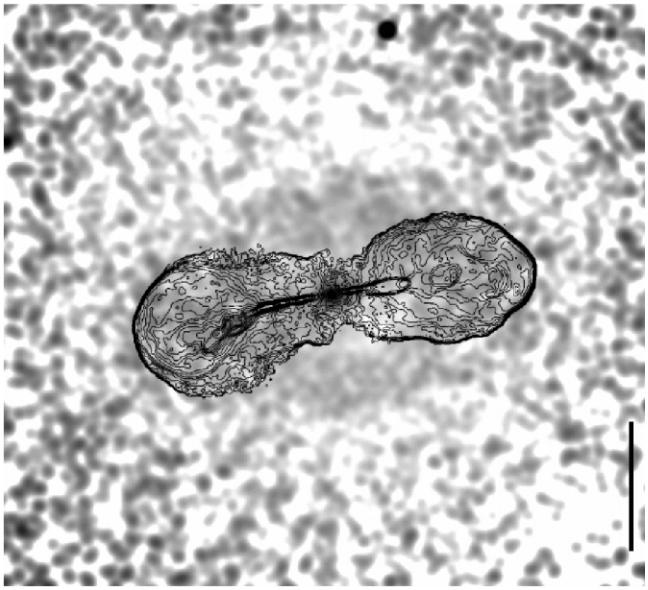

FIG. 2.—X-ray and radio images of Hercules A. The *Chandra* image of Fig. 1 is overlaid with 1.4 GHz radio contours from Gizani & Leahy (2003).

bounds this region is shown to be consistent with a shock front below.

There is an ∼7 σ deficit of X-ray emission in the region ∼0.′5 to the southwest of the bright center in Figure 1, ∼15″ (40 kpc) in radius. There is a weaker, ∼3 σ, deficit in the X-ray emission from the corresponding region to the northeast, partly masked by a bright spot of X-ray emission to the north of the center. These features resemble the cavities associated with many other cluster radio sources (e.g., McNamara et al. 2000; Fabian et al. 2000). However, they are not aligned with the axis of the radio jets and do not contain radio lobes. They might be ghost cavities (e.g., McNamara et al. 2001), but, if so, it is surprising that they lie within an active radio source.

Finally, there is a ridge of enhanced X-ray emission crossing the bright region, from ∼30° south of east to ∼30° north of west, roughly at right angles to the axis defined by the cavities. This feature also has no obvious association with the radio source (it forms an angle of ∼20° with the radio jets). The excess emission appears to be thermal, due to relatively cool, dense gas, which cannot be fully supported by hydrostatic forces. The gas may be cool filaments, like those seen in other cluster central radio sources (e.g., Forman et al. 2005; Nulsen et al. 2005), or it may be a cooler disk that is partly supported by rotation.

4. THE SHOCK FRONT IN HERCULES A

The surface brightness profile of the bright circular region was measured in two 80° sectors, approximately at right angles to the axis of the radio jet. This avoids smearing the edge in the surface brightness profile due to elongation of the bright region to the east and west. Figure 3 shows the radial surface brightness profile for the ranges of position angle (P.A.) 330°–50° and 150°–230° combined. Point sources were eliminated, the background was subtracted, and the resulting profile exposure corrected. Although the data are quite noisy, there is a clear break in surface brightness at a radius of 60″ (∼160 kpc), at the edge of the bright central region. Beyond the break, the surface brightness is well fitted by the power law, $r^{-\alpha}$ with

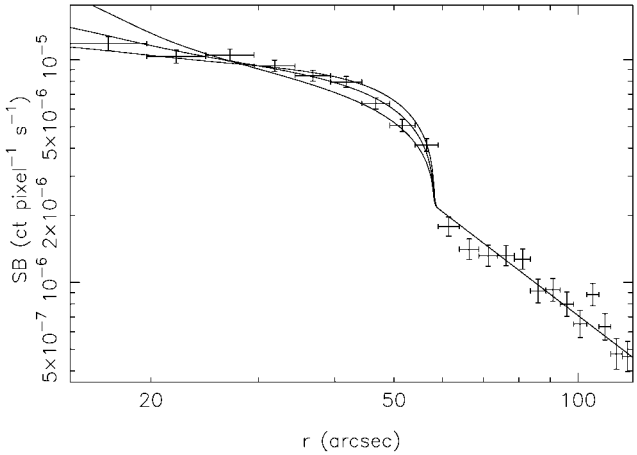

FIG. 3.—Surface brightness profile of the shock front in Hercules A. The 0.6–7.5 keV surface brightness profile is measured in sectors from P.A. 330° to 50° and from P.A. 150° to 230°, to the north and south of the AGN, at right angles to the jet axis. Surface brightness errors are 1 σ statistical errors. Radial error bars show the limits of the bins. The smooth curves are surface brightness profiles for shock models with Mach numbers of 1.51, 1.65, and 1.79, from bottom to top on the right. Models are scaled to match the observed surface brightness outside the shock.

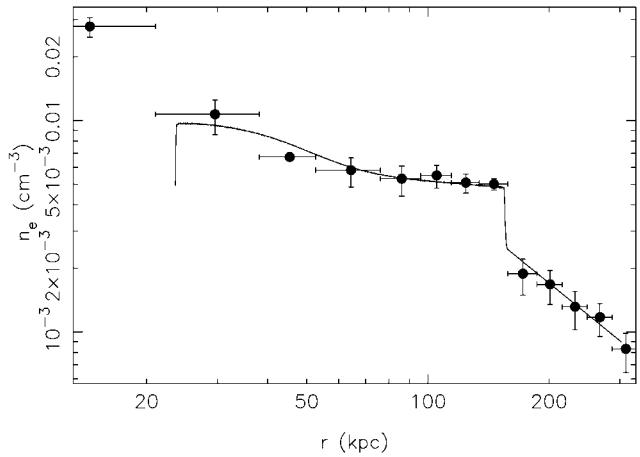

FIG. 4.—Electron density profile of the shock front in Hercules A. Deprojected electron density vs. radius in the P.A. ranges 330°–50° and 150°–230°. The shock is at 158 kpc. Density error bars are 90% confidence ranges. The solid line shows the density profile for the best-fitting model.

$\alpha = 2.11 \pm 0.43$ (90%). We now consider the interpretation of this front as a shock.

To determine the strength of the shock we use a spherically symmetric, hydrodynamic model of a point explosion at the center of an initially isothermal, hydrostatic atmosphere. Before passage of the shock, the gas density is assumed to follow the power law, $\rho(r) \propto r^{-\eta}$, with $\eta = 1.55$, chosen to make the surface brightness profile of the undisturbed gas match the observed profile outside the shock. The gravitational field ($g \propto 1/r$) is scaled to make the undisturbed atmosphere hydrostatic. The surface brightness profile is determined from the model, assuming that the temperature of the unshocked gas is 4 keV (see below). Relative *Chandra* count rates in the 0.6–7.5 keV band are computed using detector response files from near to the aim point for these observations. The XSPEC WABS × MEKAL spectral model was used, with a foreground column density of 6.4×10^{20} cm^{-2}, a redshift of 0.154, and abundances of 0.5 times solar, appropriate for Hercules A (model surface brightness profiles are insensitive to these and the preshock temperature in the relevant temperature range). The model is self-similar, allowing it to be scaled in radius to match the location of the shock and in normalization to match observed surface brightness outside the shock.

In Figure 3 we show surface brightness profiles for model shocks with Mach numbers of 1.51, 1.65, and 1.79. A Mach 1.65 shock gives a reasonable fit to the data. Apart from the scaling, model parameters (the initial density power law, η, and preshock temperature) are constrained by observations, leaving only the Mach number of the shock free in the fit. The model has a number of shortcomings (the actual outburst is aspherical and does not inject energy in a single explosion, and the initial gas density is not a power law; Nulsen et al. 2005), so that it can only be expected to match the data over a limited range of radius behind the shock. Nevertheless, the fit provides a stringent test that this feature is due to a shock propagating into the cluster.

In order to determine the physical properties of the outburst from the model, we must determine the density and temperature of the unshocked gas. However, outside the shock from 1′ to 2.′5, in the sectors of the surface brightness profile, there are only ∼1250 photons in the 0.6–7.5 keV band. We have therefore used a single spectrum extracted from this region to determine the temperature and normalize the density of the unshocked gas. Using an absorbed MEKAL model, with $N_{\rm H} = 6.4 \times 10^{20}$ cm^{-2}, redshift $z = 0.154$, and the abundance set to 0.5, gives a temperature of $kT = 3.9^{+0.8}_{-0.6}$ keV (90%). This is consistent with previous measurements (e.g., Gizani & Leahy 2003), suggesting that the spectrum is not significantly affected by the particle background. Assuming that the gas is spherically symmetric and its density $\rho(r) \propto r^{-1.55}$ from the shock to infinity, the normalization of the spectral fit gives an electron density of $n_e = 1.06 \pm 0.03 \times 10^{-3}$ cm^{-3} at a radius of 276 kpc (1.′72).

Using these parameters, the radius of the shock is 158 kpc, the time since the outburst is $t_s = 5.9 \times 10^7$ yr, and the total energy of the outburst is $E_s = 3 \times 10^{61}$ ergs. This energy is similar to the lobe enthalpy (Gizani & Leahy 2004), as expected if the lobes drive the shock. The main source of uncertainty in the age of the outburst (∼10%) is due to the uncertainty in the preshock temperature. The shortcomings of the model do give rise to systematic uncertainty in the shock energy, but this is unlikely to be more than a factor of ∼2 (Nulsen et al. 2005).

In the temperature range 1.6–10 keV, the *Chandra* count rate in the band 0.6–7.5 keV is very insensitive to gas temperature, varying ±3.3% about its mean over the whole range of temperature, for a fixed emission measure. This enables us to deproject the gas density with reasonable accuracy, despite poor knowledge of the gas temperature (doubling the abundance to 1.0 would reduce the electron density by ∼7%). A deprojection was done, using the method of Nulsen et al. (2005), with the gas temperature fixed at 4 keV and other parameters as above. The resulting electron density profile is shown in Figure 4, together with the electron density profile obtained from the Mach 1.65 shock model. The results agree well with the model, clearly showing the density jump at the shock. The failure of the model for $r \lesssim 25$ kpc is a numerical artifact, but other shortcomings are expected to make the model inaccurate at small radii.

In the models, adiabatic expansion limits the size of the

region where the temperature of the shocked gas exceeds that of the unshocked gas. Nevertheless, the strength of the shock in Hercules A makes it a good candidate for detecting the temperature rise due to the shock. For the Mach 1.65 model, after projection onto the sky, the emission measure–weighted temperature exceeds the preshock temperature by at least 20% for 110 kpc $< r <$ 150 kpc. With other fit parameters as above, a spectrum extracted from this region (~900 0.6–7.5 keV source counts) gives a temperature of $kT = 6.1^{+2.0}_{-1.2}$ keV (90%), in reasonable agreement with the model.

5. DISCUSSION

The mean power of the outburst in Hercules A, $P_s = E_s/t_s = 1.6 \times 10^{46}$ ergs s^{-1}, is 2 orders of magnitude larger than the total power radiated from the region where the cooling time is shorter than 10^{10} yr. Hercules A joins a small collection of cooling flow clusters known to have large-scale shocks driven by an outburst from an AGN at the cluster center (Fabian et al. 2003; Forman et al. 2005; McNamara et al. 2005; Nulsen et al. 2005). Three of these systems, Hydra A, MS 0735.6+7421, and Hercules A, have outburst energies of $\gtrsim 10^{61}$ ergs. The outburst in Hercules A currently has the strongest shock, and its total energy is the second largest known (MS 0735.6+7421 is twice as energetic; McNamara et al. 2005). Along with the other systems, it has important implications for the energetics of cooling flows, the preheating of clusters, the interaction of radio sources with the ICM, and the growth of nuclear black holes (McNamara et al. 2005; Nulsen et al. 2005).

If the outburst is powered by accretion onto a black hole, then the outburst energy is $E_s = \epsilon M_s c^2$, where the mass M_s was accreted to fuel the outburst and ϵ is the efficiency of jet energy production by the black hole. Unless $\epsilon > 10\%$, the mass swallowed by the black hole exceeds $1.7 \times 10^8\ M_\odot$ to fuel this outburst. If this mass was swallowed in a time comparable to the age of the outburst, $t_s \simeq 6 \times 10^7$ yr, the mass increase is hard to reconcile with a tight correlation between bulge properties and black hole mass (Gebhardt et al. 2000), unless the black hole is very massive indeed.

In our Mach 1.65 model, the shock inverts the entropy profile of gas inside 58 kpc (22″), creating a buoyant bubble at the cluster center that would then rise. A large bubble can rise at a significant fraction of the sound speed (Churazov et al. 2001), but always more slowly than the shock front. Although the shock model is not expected to match reality closely, the cavities in Hercules A are comparable in size to the entropy inversion of the model, suggesting that this is how they were formed. This would explain the lack of radio emission from the cavities.

6. CONCLUSIONS

Analysis of a *Chandra* X-ray image of the Hercules A cluster shows that it has cavities and a shock front associated with the powerful radio source. Unusually, the cavities show no clear connection to the radio source. The shock front is elongated in the direction of the radio lobes and appears to be its cocoon shock. Fitting a simple hydrodynamic model to the surface brightness profile gives a Mach number for the shock of $\simeq$1.65. The age of the outburst that drove the shock is 5.9×10^7 yr, and its total energy is 3×10^{61} ergs. The deprojected density profile is consistent with the shock model and, in particular, with the density jump at the shock. Within the limits of the spectroscopic data, the temperature jump is also consistent with the shock model.

The shock outburst is highly significant for the energetics of any cooling flow in Hercules A and for the cluster as a whole. The mean mechanical power of the outburst is $\simeq 1.6 \times 10^{46}$ ergs s^{-1}, well in the range of quasar luminosities. The black hole in the AGN that drove this outburst grew by, at least, $1.7 \times 10^8\ M_\odot$ during the outburst.

We gratefully acknowledge the assistance of Alexey Vikhlinin and Maxim Markevitch in reducing the *Chandra* data and the referee, Martin Hardcastle, for helping to improve the Letter. P. E. J. N. was partly supported by NASA grant NAS8-01130. We acknowledge support from Long Term Space Astrophysics grant NAG5-11025, *Chandra* Archival Research grant AR2-3007X, and contract 81305-001-034V from the Department of Energy through the Los Alamos National Laboratory.

REFERENCES

Birzan, L., Rafferty, D. A., McNamara, B. R., Wise, M. W., & Nulsen, P. E. J. 2004, ApJ, 607, 800
Carilli, C. L., Perley, R. A., & Harris, D. E. 1994, MNRAS, 270, 173
Churazov, E., Brüggen, M., Kaiser, C. R., Böhringer, H., & Forman, W. 2001, ApJ, 554, 261
Churazov, E., Sunyaev, R., Forman, W., & Böhringer, H. 2002, MNRAS, 332, 729
Dreher, J. W., & Feigelson, E. D. 1984, Nature, 308, 43
Fabian, A. C. 1994, ARA&A, 32, 277
Fabian, A. C., et al. 2000, MNRAS, 318, L65
Fabian, A. C., Sanders, J. S., Allen, S. W., Crawford, C. S., Iwasawa, K., Johnstone, R. M., Schmidt, R. W., & Taylor, G. B. 2003, MNRAS, 344, L43
Forman, W., et al. 2005, ApJ, in press (astro-ph/0312576)
Gebhardt, K., et al. 2000, ApJ, 539, L13
Gizani, N. A. B., & Leahy, J. P. 2003, MNRAS, 342, 399
———. 2004, MNRAS, 350, 865
Heinz, S., Reynolds, C. S., & Begelman, M. C. 1998, ApJ, 501, 126
McNamara, B. R., et al. 2000, ApJ, 534, L135
———. 2001, ApJ, 562, L149
McNamara, B. R., Nulsen, P. E. J., Wise, M. W., Rafferty, D. A., Carilli, C., Sarazin, C. L., & Blanton, E. L. 2005, Nature, 433, 45
Motl, P. M., Burns, J. O., Loken, C., Norman, M. L., & Bryan, G. 2004, ApJ, 606, 635
Narayan, R., & Medvedev, M. V. 2001, ApJ, 562, L129
Nulsen, P. E. J., McNamara, B. R., Wise, M. W., & David, L. P. 2005, ApJ, in press (astro-ph/0408315)
Peterson, J. R., Kahn, S. M., Paerels, F. B. S., Kaastra, J. S., Tamura, T., Bleeker, J. A. M., Ferrigno, C., & Jernigan, J. G. 2003, ApJ, 590, 207
Scheuer, P. A. G. 1974, MNRAS, 166, 513
Siebert, J., Kawai, N., & Brinkmann, W. 1999, A&A, 350, 25
Tabor, G., & Binney, J. 1993, MNRAS, 263, 323
Trussoni, E., Feretti, L., Massaglia, S., & Parma, P. 2001, A&A, 366, 788
Tucker, W., & David, L. P. 1997, ApJ, 484, 602
White, D. A., Jones, C., & Forman, W. 1997, MNRAS, 292, 419